frontiers | Frontiers in Earth Science

TYPE Original Research
PUBLISHED 26 July 2022
DOI 10.3389/feart.2022.960677

OPEN ACCESS

EDITED BY
Jingren Zhou,
Sichuan University, China

REVIEWED BY
Yunfeng Zhou,
Universitat Politecnica de Catalunya, Spain
Yang Lu,
Hohai University, China

*CORRESPONDENCE
Guangzhong Hu,
hgzss1983@163.com

SPECIALTY SECTION
This article was submitted to Geohazards and Georisks, a section of the journal Frontiers in Earth Science

RECEIVED 03 June 2022
ACCEPTED 30 June 2022
PUBLISHED 26 July 2022

CITATION
Hu G, Wang L, Bai J, Ma S and Tang Y (2022), Calculating the shear strength of a rock mass joint surface considering cyclic shear deterioration.
Front. Earth Sci. 10:960677.
doi: 10.3389/feart.2022.960677

Calculating the shear strength of a rock mass joint surface considering cyclic shear deterioration

Guangzhong Hu[1,2,3]*, Lijuan Wang[3], Jun Bai[1], Song Ma[3] and Yao Tang[3]

[1]State Key Laboratory of Geohazard Prevention and Geoenvironment Protection, Chengdu University of Technology, Chengdu, China, [2]College of Environment and Civil Engineering, Chengdu University of Technology, Chengdu, China, [3]Major Hazard Measurement and Control Key Laboratory of Sichuan Province (Sichuan Academy of Safety Science and Technology), Chengdu, China

The dynamic response of rock mass is largely restricted by its joint surface. Previous studies have shown that the degradation of joint surface can not be ignored when calculating the shear strength of structural plane under cyclic load. Although several studies have attempted to calculate the cyclic shear strength of a rock mass joint surface, an established and reliable method for calculating the cyclic shear strength of rock mass discontinuities is still lacking, thus necessitating further research. In this study, the deterioration effect of the shear strength of the joint surface under cyclic shearing was first analysed using cyclic shearing tests. The influence of vibration degradation in rock mass on the structural surface, undulant angle equation of the joint surface, and calculation method for the basic friction angle under a cyclic shearing load are proposed. Furthermore, the calculation method for the shear strength of the structural surface under the action of cyclic shearing is established. The proposed method is further validated through case analysis. The influence of the cutting and filling (produced during the shearing process) on the shear strength of the joint surface cannot be disregarded. The improved model proposed in this study is in good agreement with the experimental results; however, when the improved proposed method is used to estimate the cyclic shear strength of the joint surface where the normal stress is too large, calculation results may contain certain errors.

KEYWORDS

degradation effect, undulant angle, basic friction angle, shear strength, joint surface

1 Introduction

The rock mass joint surface is a two-dimensional geological interface with a particular direction, large extension, and small thickness of various structural relics (including faults, joints, bedding, and fractured zones) produced in the rock mass under the action of tectonic stress. The dynamic response of a rock mass is largely restricted by its joint surface (Wang and Zhang, 1982; Fox et al., 1998; Siad 2003; Liu 2017; Hu et al., 2020; Cui et al., 2021; Fw et al., 2021; Zhang et al., 2021). Therefore, the study of the dynamic characteristics of the joint surface, especially the dynamic shear characteristics, is an important prerequisite for the analysis of the dynamic response of a rock mass. Generally, seismic load is both dynamic and cyclic, and when a rock slope is under dynamic cyclic shearing action, the strength of its joint surface is reduced (Jafari et al., 2003; Barla et al., 2010; Woo et al., 2010; Atapour and Moosavi, 2014; Barton 2020; Zhou et al., 2021; Han et al., 2022), thereby easing the dislocation and slip of the slope along the joint surface (particularly the bedding rock slope), and resulting in geological disasters (Bhasin et al., 2004; Huang and Li, 2009; Moriya et al., 2010; Cui et al., 2013; Chen et al., 2020; Li et al., 2021a, 2021b, Li 2022a; Li 2022b). Therefore, the strength degradation and deformation mechanism of the rock mass joint surface under dynamic cyclic shear load is an essential scientific issue that needs to be addressed for the prevention and control of engineering earthquakes.

Experimental research on the mechanical behaviour of a rock mass forms the basis for the development of its constitutive model. Several studies have used physical tests to investigate the mechanical properties of structural surfaces under cyclic shear loads. For example, Jafari et al. (2003) used cement mortar to produce regular zigzag and natural joint surfaces in batches. Moreover, they analysed the shear characteristics of rock mass structural surfaces that exhibited changes in normal load, cyclic shear number, and shear rate. Fathi et al. (2016) fabricated natural unweathered granite structural surfaces with varying degrees of undulation using cement mortar and carried out cyclic shear tests. They found that the roughness and shear parameters of the joint surface decreased following an increase in the number of shear cycles. Xia et al. (2012) conducted cyclic shear tests on joint surfaces under different normal stresses and found that as the normal stress increased, the peak shear strength of the same route in the same cycle increased. In addition, the shear strength of the rock joint surface decreased as the cyclic shearing times increased. Premadasa et al. (2012) conducted cyclic shear tests on rock mass joint surfaces and showed that joint surfaces gradually transitioned from slip failure to shear failure following an increase in normal stress. Furthermore, they observed that the shear strength of the rock mass joint surface decreased as the number of cyclic shearing cycles increased and the shear failure of the joint surface mainly occurred in the initial shearing stage. Mirzaghorbanali et al. (2014) conducted cyclic shear tests with different normal stresses and shear rates on artificially fabricated joint surfaces and discussed the failure characteristics of joint surfaces in detail. Qu (2018) used cement mortar to replicate shear joint surfaces and split joint surfaces in batches, and studied the evolution characteristics of shear stress and normal displacement of different joint surfaces through cyclic shear tests. The cyclic shear testing of the various rock mass joint surfaces showed that their degradation under cyclic loads is complex, and that the performance degradation is mainly reflected as follows: 1) under the cyclic shear of the seismic load, the undulant angle decreases, and 2) under a dynamic load, the friction coefficient of the structural surface is reduced.

The accurate evaluation of the shear strength of rough rock joints has been a constant pursuit among rock mechanics research workers (Xie et al., 2022). Researchers have proposed various shear constitutive models for cyclic and dynamic load conditions based on test results and the elastoplastic theory. Plesha (1987) proposed that the joint surface undulant angle gradually degenerates under cyclic shear loading. Huang et al. (1993) performed cycle tests on sawtooth samples and verified the degradation law proposed by Plesha (1987). Qiu et al. (1993) regarded structural surface wear as plastic deformation and proposed a function of tangential plastic work as an index for expressing wear. Furthermore, they established an elastoplastic constitutive model considering the dilatancy angle and wear parameters. Divoux et al. (1997) proposed a cyclic shear mechanics constitutive model for joint surfaces based on the results of numerous cyclic shear tests. Homand et al. (2001) studied the dilatation and wear characteristics of the joint surface during the cyclic shearing process of an artificial granite joint surface using cyclic shear tests. The empirical formula for the cyclic shear strength of the rock mass joint surface was proposed by fitting. Lee et al. (2001) performed in-depth analysis of the evolution characteristics of shear stress and normal displacement through the cyclic shear test of the rough joint surface of the rock mass, and proposed a cyclic shear elastic-plastic constitutive model. Liu et al. (2013) comprehensively analysed the deformation failure characteristics and peak shear strength degradation effect of joint surfaces during the cyclic shearing process through experiments, and proposed a formula for calculating the cyclic shear strength of joint surfaces based on the test data. Mroz and Giambanco. (2015) described microscopic effects such as debonding, slippage, and dilatancy of the micro convex body through the interaction of spherical structural surfaces and proposed a constitutive model that can effectively simulate the softening phenomenon after the first cycle. While these studies have contributed significantly to the calculation of the cyclic shear strength of rock mass discontinuities, the methods used have neither been verified nor established as reliable, and should be studied further.

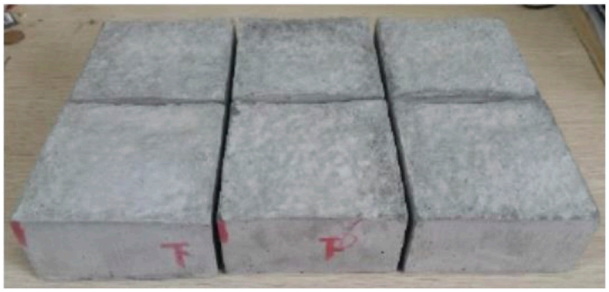

FIGURE 1
Upper and lower parts of the splitting structural plane (Qu 2018).

FIGURE 2
Anastomotic splitting structural plane (Qu 2018).

In this study, the deterioration of the shear strength of a joint surface under cyclic shearing was analysed using cyclic shearing tests. The influence of vibration degradation in rock mass on the structural surface, undulant angle equation of the joint surface, and calculation method for the basic friction angle under a cyclic shearing load are proposed. A calculation method for the shear strength of the joint surface under the action of cyclic shearing is established. The results of this study are expected to provide a theoretical basis for the stability analysis of rock slopes under seismic loads.

2 Cyclic shear testing of the joint surface

2.1 Experimental method

Numerous studies have shown that the artificial sawtooth structure in the cyclic shear test can reflect the deformation and failure characteristics of the structure during the shearing process to a certain extent. However, this structure cannot accurately reflect the change in the joint roughness coefficient (JRC) of the joint surface. In this study, cyclic shear tests of sandstone split joint surfaces (Figures 1, 2) carried out by Qu (2018) were used to illustrate the deterioration in the shear strength of the joint surfaces during cyclic shearing. The split joint surfaces of the sandstone were replicated using plain concrete with a cement:sand:water mass ratio of 3:2:1. Table 1 lists the basic mechanical parameters of plain concrete and sandstone, showing that the selected materials have mechanical properties that are similar to those of sandstone (Qu 2018; Dong et al., 2020).

Based on the direct shear test of 136 joint surfaces, Barton and Choubey (1977) found that when the shear strength decreased to its residual strength, the shear displacement was approximately 10% of the length of the structural surface. Furthermore, considering the maximum shear displacement limit of the test device, the target shear displacement was set to 10% of the length of the joint surface. The total length of the joint surface sample was 100 mm; therefore, the shear target displacement was ±10 mm. Cyclic shear tests on split joint surfaces with normal stresses of 3, 6, and 9 MPa were performed using a coal rock shear-flow coupling test device that was independently developed at Chongqing University (Xu et al., 2015). During the test, the upper shear box was fixed and the route division was based on the shear displacement of the lower shear box. Subsequently, the lower shear box was fixed and the route division was based on the shear displacement of the upper shear box. A complete cyclic shear process consists of four routes, which is shown in Figure 3.

2.2 Deterioration in shear strength

2.2.1 Analyses of shear stress-displacement curves

As shown in Figure 4, in route 1 of cycle 1, the shear stress-displacement curve of the joint surface is mainly a peak curve, which indicates that the joint surface primarily undergoes shear failure. In the subsequent shear process, the shear stress-displacement curve of the joint surface is a slip curve, and the shear stress remains unchanged. This is because the slip and wear damage between the contact surface, cutting filling, and cuttings is the major cause of the subsequent shearing process. The deterioration in the shear strength of the joint surface under cyclic shear was mostly reflected in the first cyclic shear. Furthermore, as the normal stress increased, the slope of the elastic deformation stage increased before the shear stress reached its peak value (when the shear modulus increased). After the peak value, the rate of decrease in shear stress also increased, thus indicating that the shear failure characteristics of the joint surface become increasingly evident as the normal stress increases.

TABLE 1 Mechanical parameters of sandstone and similar materials (Qu, 2018).

Material	Density ($g \cdot cm^{-3}$)	Uniaxial compressive strength (MPa)	Cohesion (MPa)	Friction angle (°)	Elastic modulus (GPa)	Poisson's ratio
Sandstone	2.32	81.04	11.52	67.18	6.79	0.26
Similar materials (Plain concrete)	2.05	77.57	14.37	62.39	6.35	0.24

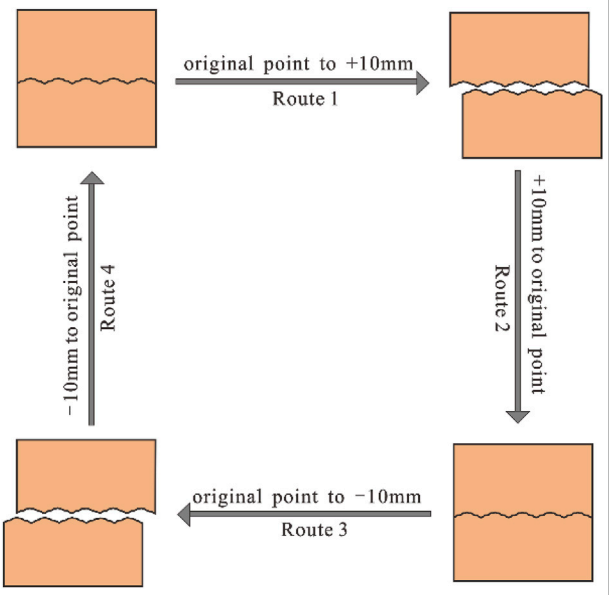

FIGURE 3
Route divisions of a single shear cycle (Qu 2018; Dong et al., 2020).

2.2.2 Analyses of normal displacement-shear displacement curves

The normal displacement-shear displacement curves are shown in Figure 5, where the normal stress increases, maximum normal dilatancy displacement decreases, and shear shrinkage displacement increases. This is because as normal stress increases, the initial shear failure (especially in route 1) in the shear process of the joint surface becomes increasingly evident, and the degree of wear gradually intensifies in the subsequent shearing process, resulting in smaller particles, reduced volume, and lower filling height of the rock debris. In addition, following an increase in shear time, the lower the normal stress, the higher the overlap of the normal-shear displacement curves. This is because as the number of cyclic shear cycles increases, the degree of wear of the joint surface in each shearing process decreases. After multiple cyclic shears, the joint surface wear is gradually stabilised. Therefore, the lower the normal stress, the sooner the joint surface wear stabilises.

2.2.3 Deterioration of shear strength with an increase in cyclic shear times

Liu et al. (2011); Liu et al. (2013) defined the shear strength ratio of the joint surface. The joint surface shear strength ratio (D_n, ranging between 0.0 and 1.0) refers to the ratio of the peak shear strength of the n-th shear cycle (τ_n) to the peak shear strength of the first shear cycle (τ_1).

$$D_n = \frac{\tau_n}{\tau_1} \tag{1}$$

The closer D_n is to 1, the lower the strength deterioration caused by the cyclic shear of the joint surface. The smaller the value of D_n, the greater the strength deterioration caused by the cyclic shear of the joint surface. Figure 6 shows the changes in the shear strength ratios of the joint surfaces under different normal stresses with cyclic shear times. The results show that as normal stress increases, the rate of decrease in the shear stress rate increases. However, generally, the test results show that under the action of different normal stresses, the variation trend of the joint surface shear strength ratio (D_n) is essentially the same. Moreover, as the cyclic shear time increases, the shear stress ratio decreases gradually and tends to stabilise. This also proves that the shear failure of the joint surface is mainly generated in the first two shearing processes, and the subsequent shearing processes are mainly caused by slip and wear damages among the contact surface, cutting filling, and cuttings.

3 Shear strength of the rock mass joint surface under cyclic shear

The mechanism of the joint surface in the shearing process is relatively complex, and several factors contribute to its shear strength. For ordinary joint surface shear tests (without considering cyclic shear), the relationship curve between the shear stress and the normal stress of the joint surface is shown in Figure 7. In the initial stage of shearing, the joint surface mainly exhibits dilation, and as normal and shear stresses increase, part of the protrusions on the joint surface is sheared off until the plane reaches the peak strength. For the shear strength of the joint surface, Newland and Allely (1957) developed the following equation:

$$\tau = \sigma_n tan(\varphi_b + i) \tag{2}$$

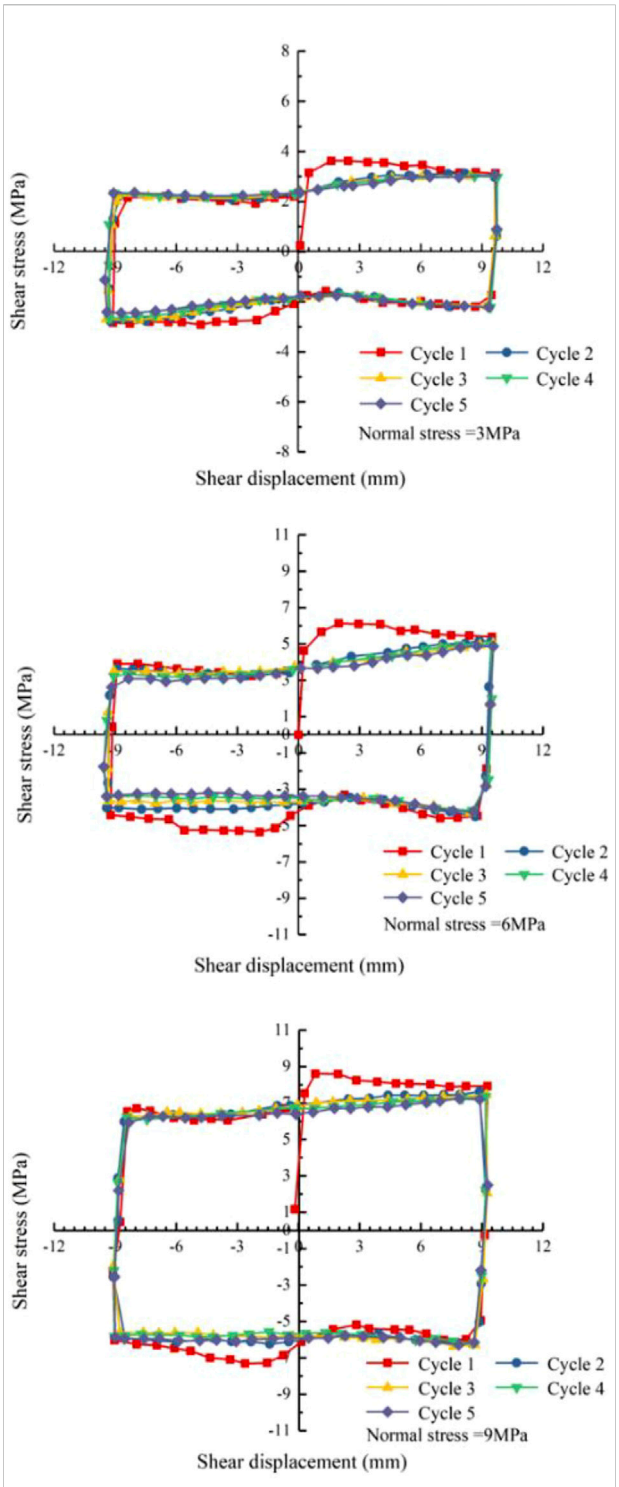

FIGURE 4
Shear stress-displacement curve of the structural plane under different normal stresses (Qu 2018; Dong et al., 2020).

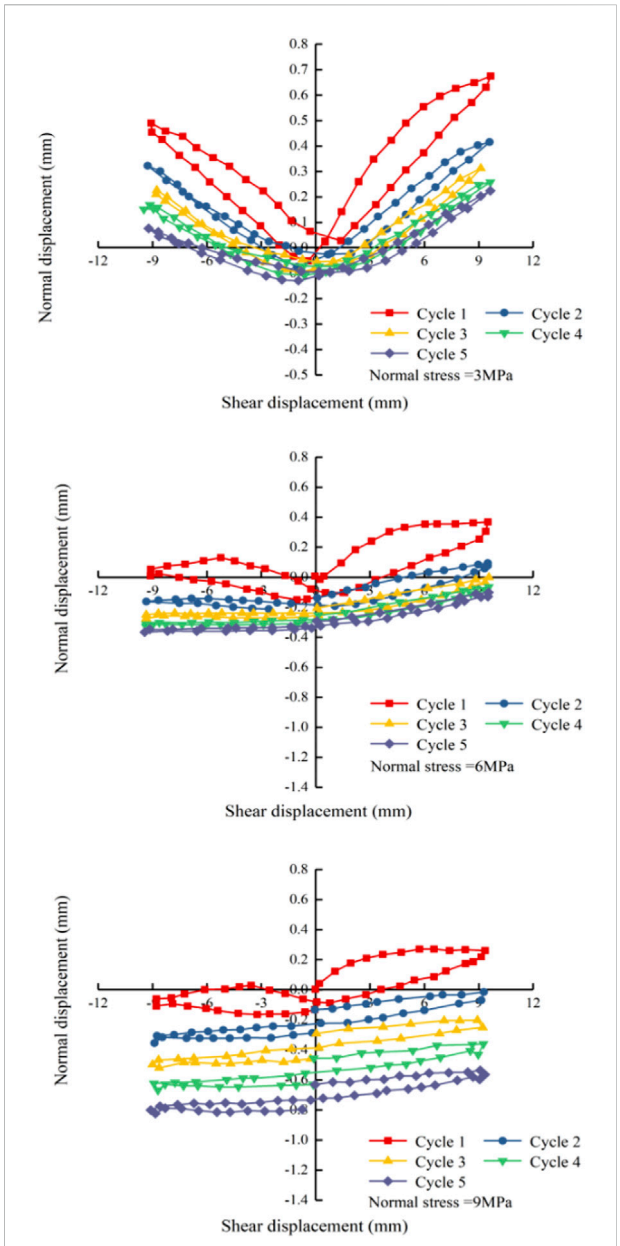

FIGURE 5
Normal displacement-shear displacement curve of the structural plane under different normal stresses (Qu 2018; Dong et al., 2020).

where σ_n is the effective normal stress, i is the average angle of deviation of particle displacements from the direction of the applied shear stress, and φ_b is the angle of frictional sliding resistance between the particles. Patton (1966a); Patton (1966b) and Goldstein et al. (1966) used Eq. 2 to represent the shear strength of irregular rock surfaces and broken rock when tested at low normal stresses. At high normal stresses, the Coulomb relationship is assumed to be as follows

$$\tau = c + \sigma_n tan\varphi. \quad (3)$$

where τ is the shear stress, c is the cohesion force, σ_n is the normal stress, and φ is the friction angle.

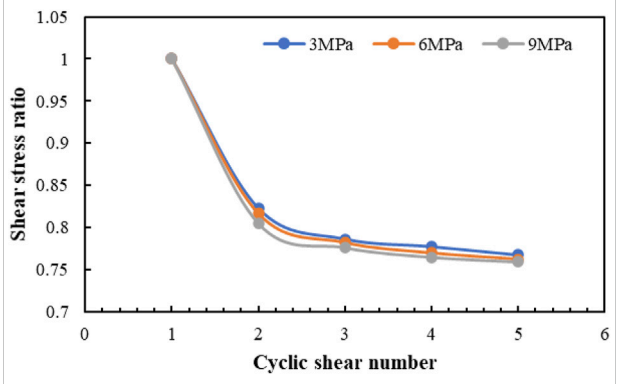

FIGURE 6
Change in shear strength ratio of the structural plane with cyclic shear times under different normal stress levels.

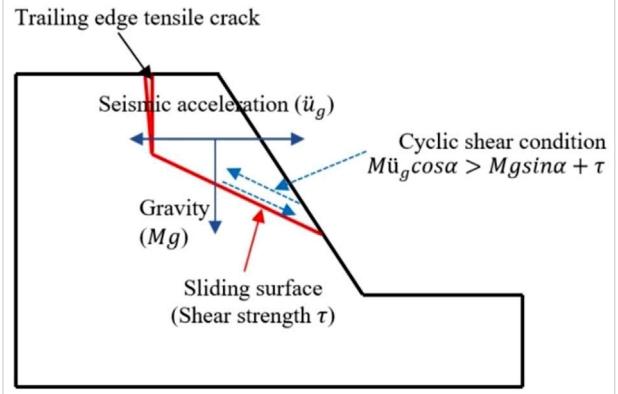

FIGURE 8
Stress diagram of a bedding rock sliding mass under a horizontal earthquake.

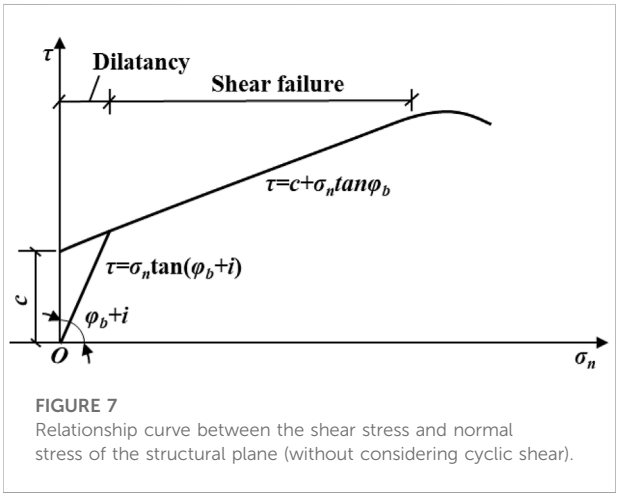

FIGURE 7
Relationship curve between the shear stress and normal stress of the structural plane (without considering cyclic shear).

According to the test results, the shear failure of the joint surface occurs primarily in route 1 of cycle 1, and the cohesion force (c) should only be considered prior to the first shear process. Dong et al. (2020) proposed that in the analysis of slope stability under seismic loads, when the upward component of the horizontal seismic force ($M\ddot{u}_g cos\alpha$) exceeds the combined force of the shear strength of the interlayer joint surface and the weight component of the sliding body ($Mgsin\alpha$), the slipping body enters a cyclic shear mode (Figure 8). Therefore, the cohesion term should only be considered prior to the first sliding event, and the contribution of cohesion is commonly disregarded in practical calculations. Therefore, under cyclic loading, the shear strength of the rock mass joint surface can be expressed as follows

$$\tau = \sigma_n tan\varphi \tag{4}$$

where σ_n is the normal stress and φ is the internal friction angle. While the rough undulations of most joint surfaces in natural rock masses are irregular, when a rock mass shears along the joint surface, the shear resistance of the joint surface comprises two parts: one caused by the undulation of the joint surface and the other caused by the friction of the contact parts. Therefore,

$$\varphi = \varphi_b + \alpha_k \tag{5}$$

where α_k is the undulant angle for a flat joint surface, and $\varphi = \varphi_b$ (φ_b is the basic friction angle).

Furthermore, Eq. 3 can be expressed as follows.

$$\tau = \sigma_n tan(\varphi_n + \alpha_n) \tag{6}$$

where φ_n and α_n are the basic friction angle and undulant angle of the joint surface for the n-th cyclic shear, respectively.

According to Eq. 5, when the normal stress and shear rate are constant, the shear stress is mainly affected by the undulant and basic friction angles. Therefore, clarifying the changes in the undulant angle and basic friction angle in the cyclic shear process is essential to determining the shear strength of the joint surface in the process of cyclic shear.

4 Deterioration of internal friction angle

4.1 Undulant angle of the joint surface

The surface morphology of the joint surface is a crucial factor affecting the shear failure mode, which can be explained by a study of the relationship between the undulant joint surfaces and strength. For a rock mass joint surface under a particular normal stress, the increase in the tangential displacement directly leads to a degradation of the undulant angle of the joint surface. When considering the degradation law of strength for rock mass joint

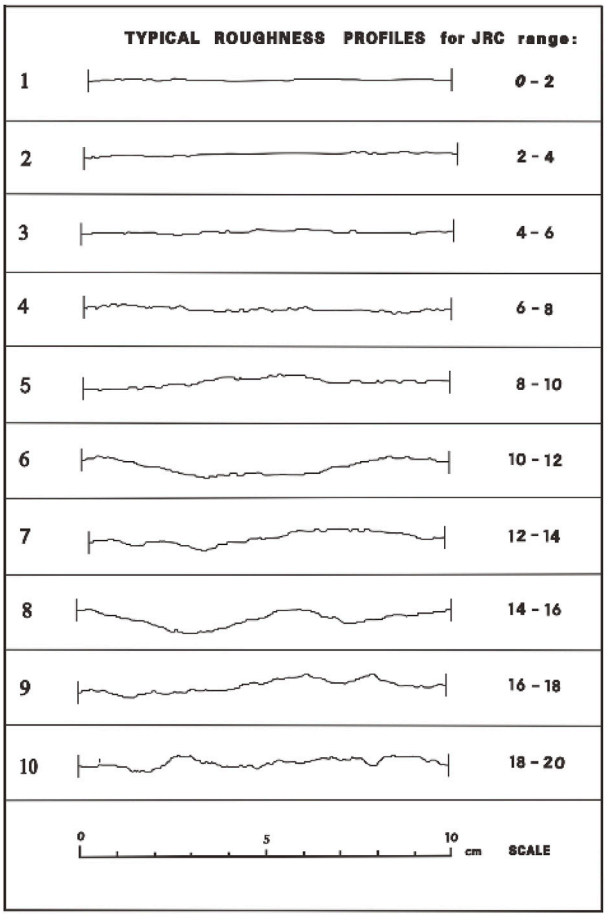

FIGURE 9
Rough joint Profliles (Barton and Choubey,1977).

surfaces under cyclic shear, the degradation phenomenon of its undulant angle during cyclic loading is typically considered. Pioneering research pertaining to the study of the degradation in the joint surface undulant angle was conducted by Plesha (1987), who proposed that the joint surface undulant angle (α_k) gradually degenerates under cyclic shear loading, and is expressed as follows

$$\alpha_k = (\alpha_k)_0 e^{-cW^p} \tag{7}$$

where $(\alpha_k)_0$ is the initial undulant angle, c is the joint surface damage coefficient, W^p is the plastic work, and τ is the shear stress.

4.1.1 Damage coefficient of the joint surface

Hutson and Dowding (1990) and Jing et al. (1993) verified the accuracy of the model proposed by Plesha (1987). By fitting a large amount of experimental data, they further proposed the following empirical calculation formula for the damage coefficient c of the joint surface:

$$c = -0.114 JRC\left(\frac{\sigma_n}{\sigma_c}\right) \tag{8}$$

where σ_c is the uniaxial compressive strength of the rock wall, σ_n is the normal stress, and JRC is the roughness coefficient of the joint surface.

In Eq. 8, the JRC is the most difficult parameter to determine. Several methods, such as the roughness parameter, non-automatic continuous measurement, fractal dimension measurement, and empirical estimation methods, have been utilised to determine the JRC of rock masses. Although the roughness parameter method exhibits high measurement accuracy, measuring a joint surface contour curve is burdensome, which is not conducive to the rapid application of the model. Moreover, non-automatic continuous measurement may lead to large errors, thereby significantly reducing accuracy. The results of practical applications indicate that the steps for estimating JRC using fractal dimension measurement methods are cumbersome and slow. Barton and Choubey (1977) presented a set of ten increasing rough joint profiles measured on 10 cm long specimens based on a large number of tests, which can be physically compared with profiles measured on other joints (Figure 9). The method proposed by Barton and Choubey (1977) has been accepted by ISRM as a standard; however, its evaluation accuracy depends on the user's experience and numerous subjective factors. A more reliable method for determining the JRC is conducting a tilt test on a jointed core. Based on the back-analysis and estimation of the results of several shear tests, Barton (1982) proposed the following equation:

$$JRC = \frac{arctan\left(\tau/\sigma_n\right) - \varphi_r}{\log_{10}\left(JCS/\sigma_n\right)} \tag{9}$$

According to Eq. 3, for the cyclic shear,

$$arctan\left(\tau_n/\sigma_n\right) = \varphi_n \tag{10}$$

Then, Eq. 10 can be expressed as follows

$$JRC = \frac{\varphi_n - \varphi_r}{\log_{10}\left(JCS/\sigma_n\right)} \tag{11}$$

where τ_n and φ_n are the shear strength and friction angle of the joint surface after the n-th cyclic shear, respectively. φ_r is the residual friction angle of the joint surface, and JCS is the rock wall compressive strength.

4.1.2 Plastic work

In cyclic loading, the tangential displacement increment produced by cyclic loading can be expressed as Δx_i. Therefore, the plastic work can be expressed as follows

$$\Delta W_i^p = |\tau \cdot \Delta x_i| \tag{12}$$

Furthermore, the cumulative tangential plastic work produced by the joint surface after n cyclic loadings is as follows:

$$\Delta W_n^p = \left|\frac{\tau_{nmax} - \tau_{nmin}}{2} \cdot \sum_1^i \Delta x_n\right| \tag{13}$$

Where ΔW_n^p is the Plastic work, Δx_i is the tangential displacement increment produced by cyclic loading, and τ_{imax} and τ_{imin} is the upper and lower limit shear stresses of cyclic loading are respectively.

4.2 Basic friction angle of the joint surface

After n cycles, if the undulation angle of the joint surface is relatively close to its initial value, the deterioration degree of the joint surface is relatively low, indicating that the basic friction angle is also relatively close to its initial value. If the difference between the undulation angle after the n-th cyclic shear and the initial undulation angle is relatively close to the residual undulation angle (final undulation angle of the joint surface after the cyclic shear test), the degree of deterioration of the structural surface is relatively high, which implies that the basic friction angle is relatively close to the residual value. The change in the basic friction angle of the n-th cyclic shear (φ_n) in the interval $[\varphi_0, \varphi_r]$ during cyclic shear was inferred to be similar to that of the dilatancy angle (α_n) in the interval $[\alpha_0, \alpha_r]$ (Dong et al., 2020). The following equation was proposed:

$$\frac{\alpha_0 - \alpha_n}{\alpha_0 - \alpha_r} = \frac{\varphi_0 - \varphi_n}{\varphi_0 - \varphi_r} \tag{14}$$

where α_n is the average dilatancy angle of the n-th cyclic shear, α_0 is the initial undulant angle, α_r is the residual undulant angle, φ_0 is the initial basic friction angle of the joint surface, φ_r is the residual basic friction angle, and φ_n is the basic friction angle of the n-th cyclic shear.

Therefore, the basic friction angle φ_n of the joint surface is expressed as follows

$$\varphi_n = \frac{\alpha_n(\varphi_0 - \varphi_r) - \varphi_0\alpha_r + \varphi_r\alpha_0}{\alpha_0 - \alpha_r} \tag{15}$$

The φ_0 can be determined based on the inclination-angle test of the smooth test block. Based on Eq. 3, the relationship between the residual friction angle (φ_s) can be expressed as follows

$$\varphi_s = \arctan\left(\tau_r/\sigma_n\right) \tag{16}$$

where σ_n is the normal stress applied during the shear process, and τ_r is the residual shear stress.

Based on Eq. 4, the residual basic friction angle is expressed as follows

$$\varphi_r = \varphi_s - \alpha_r = \arctan\left(\tau_r/\sigma_n\right) - \alpha_r \tag{17}$$

Furthermore, based on Eqs 21, 23, the basic friction angle can be determined as follows

$$\varphi_n = \frac{(\alpha_0 - \alpha_n)\left[\arctan\left(\tau_r/\sigma_n\right) - \alpha_r\right] + (\alpha_n - \alpha_r)\varphi_0}{\alpha_0 - \alpha_r} \tag{18}$$

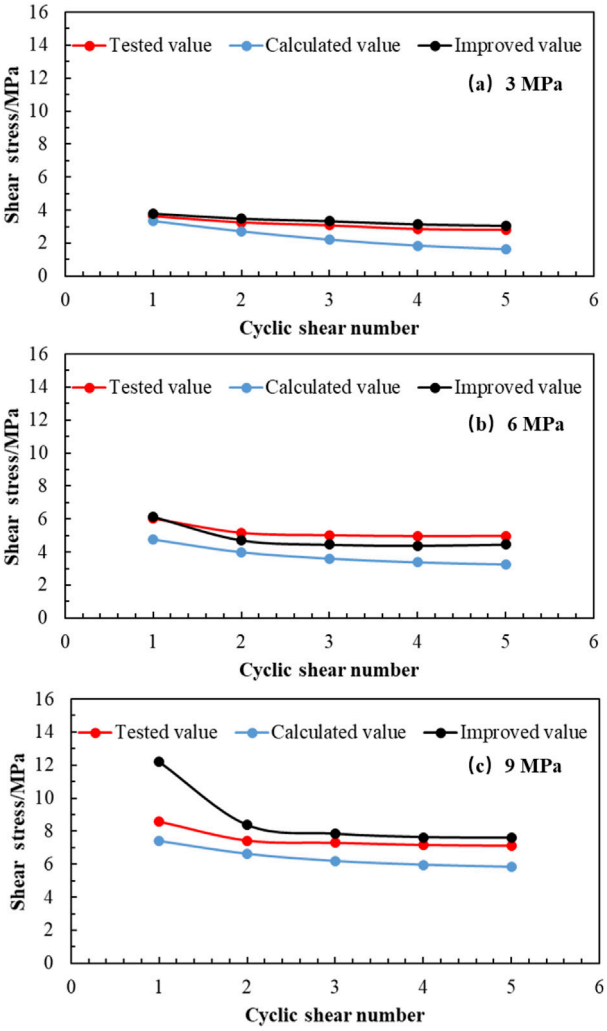

FIGURE 10
Shear stresses obtained by tests, proposed method, and improved method under different normal stress of 3, 6 and 9 Mpa.

5 Case study

5.1 Verification and improvement of the proposed method

The feasibility of the proposed method was verified using the cyclic shear test results obtained by Qu (2018) (details are presented in Section 2). The cyclic shear tests and calculation results are presented in Figure 10 and Table 2. The calculation results of the proposed method are generally lower than the experimental values. This is because the calculation method is proposed considering the ideal state, that is, without considering the effect of cuttings on the shear strength of the joint surface during the cyclic shearing process. In fact, during the shearing process, the sheared cuttings are stuffed

TABLE 2 Calculation parameters and obtained shear strengths.

Cyclic number	Normal stress/MPa	Basic friction angle/°		$\frac{\varphi_{bt}}{\varphi_{bc}}$	Shear strength		
		φ_{bt}	φ_{bc}		Test	Proposed	Improved
1	3	41.17	38.88	1.06	3.63	3.52	3.76
2		38.27	34.26	1.12	3.12	2.96	3.28
3		37.42	29.32	1.28	3.07	2.51	3.23
4		36.83	25.12	1.47	2.97	2.17	3.14
5		35.53	22.16	1.60	2.99	1.98	3.06
1	6	39.28	32.50	1.21	6.13	4.73	6.13
2		36.35	29.30	1.24	5.16	3.96	4.72
3		36.64	27.76	1.32	5.01	3.587	4.45
4		37.12	26.95	1.38	4.95	3.36	4.38
5		37.87	26.65	1.42	4.87	3.25	4.46
1	9	40.83	36.58	1.12	8.60	7.40	12.20
2		37.80	34.59	1.09	7.43	6.62	8.36
3		37.90	33.36	1.14	7.29	6.18	7.82
4		37.75	32.71	1.15	7.16	5.95	7.62
5		37.78	32.35	1.17	7.11	5.82	7.58

between the joint surfaces as fillers, causing the friction in the joint surface in the subsequent shear process, mainly generated in three parts: between two joint surfaces, between the joint surface and cuttings, and between the two sets of cuttings. The calculation results show that when calculating the cyclic shear strength of the joint surface, the influence of rock debris filling on the shear strength (especially the basic friction angle) of the joint surface must be considered.

Therefore, it is necessary to improve the calculation method for the basic friction angle. A correction coefficient (β) was introduced to improve the accuracy of the basic friction angle. The correction coefficient is defined as the ratio of the basic friction angle obtained from the test to the calculated value:

$$\beta = \frac{\varphi_{bt}}{\varphi_{bc}} \tag{19}$$

where φ_{bc} and φ_{bt} are the calculated and test basic friction angles, respectively. The basic friction angle obtained from test data and the calculated basic friction angle obtained after each shearing cycle are presented in Table 2. According to multiple fittings, the ratio of the number of shear cycles to the normal stress exhibits a suitable linear relationship with the β value (Figure 11), and the expression is as follows:

$$\beta = A\left(\frac{n}{\sigma_n}\right) + B \tag{20}$$

The values of A and B of the joint surface samples with the same intact rock strength have a linear relationship with the normal stress; therefore, the calculation formulas of parameters A and B are assumed to be as follows

$$\begin{cases} A = a\sigma_n + b \\ B = c\sigma_n + d \end{cases} \tag{21}$$

where a, b, c, and d are constants. Finally, according to the fitting (Figure 12), A and B are obtained as follows:

$$\begin{cases} A = -0.0655\sigma_n + 0.7678 \\ B = 0.0483\sigma_n + 0.6833 \end{cases} \tag{22}$$

Therefore, β can be expressed as follows.

$$\beta = (-0.0655\sigma_n + 0.7678)\frac{n}{\sigma_n} + 0.0483\sigma_n + 0.6833 \tag{23}$$

The basic friction angle under the cyclic angle can be calculated as follows.

$$\varphi_{nI} = \beta\varphi_n \tag{24}$$

where φ_{nI} denotes the basic friction angle of the n-th cyclic shear, considering the filling effect of the rock cuttings in the shear process.

5.2 Comparative analysis

Comparison between the shear stress obtained using the proposed method, improved method, and tests is shown in

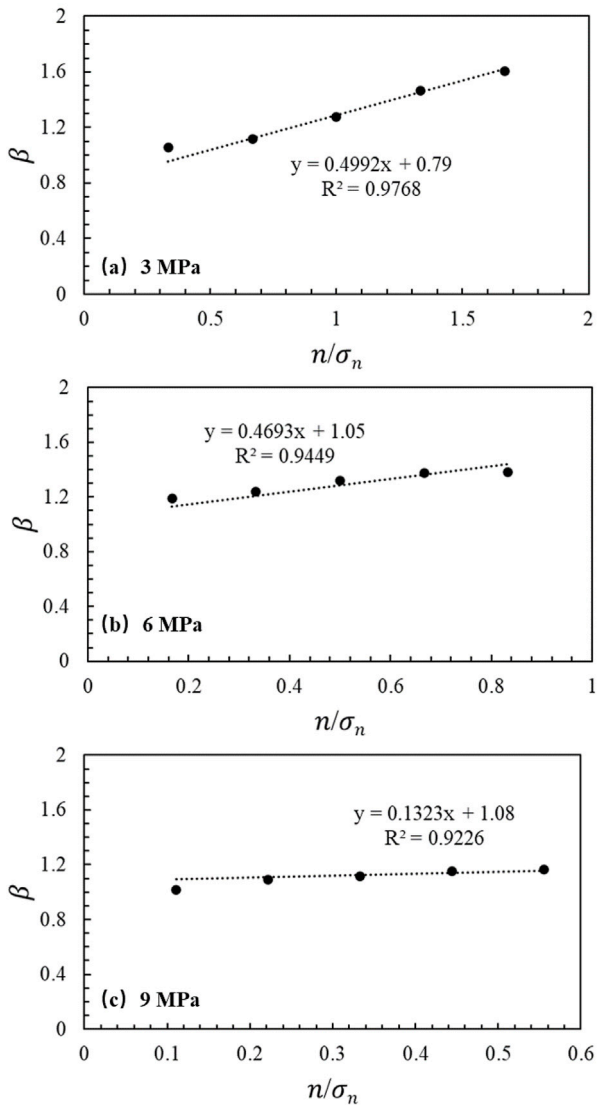

FIGURE 11
Fitting results of β and $\frac{n}{\sigma_n}$ under different normal stress of 3, 6 and 9 Mpa.

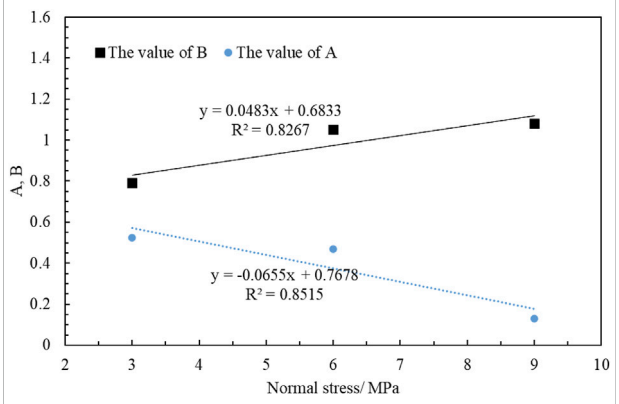

FIGURE 12
Fitting results of parameters A and B.

Figure 10. The results show that regardless of the method, the shear strength of the joint surface decreases gradually as the number of cycles increases, and that the decreasing trend gradually slows down. Compared with the proposed method, the shear stress obtained using the improved method is in good agreement with the experimental results; however, when the normal stress was 9 MPa, the shear strength in cycle 1 was considerably different from the experimental value. The failure mode of the joint surface in cycle 1 under high normal stress conditions differed from that under low normal stress conditions. Under high normal stress, the failure mode of the protrusion was tensile rather than shear, and the tensile strength of the material was the controlling factor, which is inconsistent with the assumption that the matrix material reaches shear strength and fails made in the calculation equation. Therefore, when using the calculation equation to estimate the shear strength of the joint surface in cycle 1, the normal stress should not be too large.

6 Conclusion

This study investigated the shear strength of a rock mass joint surface under cyclic loading by first examining the effect of cyclic shear deterioration, the influence of vibration degradation in rock mass on the structural surface, undulant angle equation of the joint surface, and calculation method for the basic friction angle under a cyclic shearing load are proposed firstly. And then proposing an equation for calculating the shear strength, with the following conclusions:

1) Under the action of different normal stresses, as the number of cyclic shear cycles increases, the degree of wear of the joint surface in each shearing process decreases. After multiple cyclic shears, the joint surface gradually stabilises. The lower the normal stress, the sooner the joint surface wear stabilises.
2) During the shearing process, the sheared cuttings are stuffed between the joint surfaces, and the influence of the cutting and filling (produced in the shearing process) on the shear strength of the joint surface cannot be disregarded.
3) The improved model proposed in this study is in good agreement with the experimental results; however, when the improved proposed method is used to estimate the cyclic shear strength of the joint surface where the normal stress is too large, there may be errors in the calculation results.

Data availability statement

The original contributions presented in the study are included in the article/Supplementary Material, further inquiries can be directed to the corresponding author.

Author contributions

GH and JB were responsible for writing and idea discussions; Other authors were responsible for the editing of drawings, tables, and paper language.

Acknowledgments

Thank Shan Dong et al. (2020) for providing relevant data support.

Conflict of interest

The authors declare that the research was conducted in the absence of any commercial or financial relationships that could be construed as a potential conflict of interest.

Publisher's note

All claims expressed in this article are solely those of the authors and do not necessarily represent those of their affiliated organizations, or those of the publisher, the editors and the reviewers. Any product that may be evaluated in this article, or claim that may be made by its manufacturer, is not guaranteed or endorsed by the publisher.

References

Atapour, H., and Moosavi, M. (2014). The influence of shearing velocity on shear behavior of artificial joints. *Rock Mech. Rock Eng.* 47 (5), 1745–1761. doi:10.1007/s00603-013-0481-9

Barla, G., Barla, M., and Martinotti, M. E. (2010). Development of a new direct shear testing apparatus. *Rock Mech. Rock Eng.* 43 (1), 117–122. doi:10.1007/s00603-009-0041-5

Barton, N. (1982). *Modelling rock joint behavior from* in situ *block tests: Implications for nuclear waste repository design*. Columbus, OH: Office of Nuclear Waste Isolation, 96. ONWI-308.

Barton, N. R., and Choubey, V. (1977). The shear strength of rock joints in theory and practice. *Rock Mech.* 10 (1), 1–54. doi:10.1007/bf01261801

Barton, N. (2020). The many faces of q-rock mass characterization for tunnels, caverns, slopes, tbm prognosis, deformability, shear strength, seismic velocity, permeability.

Bhasin, R., Kaynia, A., Blikra, L. H., Braathen, A., and Anda, E. (2004). Insights into the deformation mechanisms of a jointed rock slope subjected to dynamic loading. *Int. J. Rock Mech. Min. Sci. (1997).* 41 (3), 587–592. doi:10.1016/j.ijrmms.2004.03.104

Chen, Q., Liu, Y., and Pu, S. (2020). Strength characteristics of nonpenetrating joint rock mass under different shear conditions. *Adv. Civ. Eng.* 2020 (7), 1–13. doi:10.1155/2020/3579725

Cui, P., Su, Z. M., Chen, X. Q., and Zhou, J. W. (2013). *formation and risk reduction of landslide-dammed lakes resulted by the ms 8.0 wenchuan earthquake: A brief review and a proposal*. Springer Berlin Heidelberg.

Cui, S., Pei, X., Jiang, Y., Wang, G., Fan, X., Yang, Q., et al. (2021). Liquefaction within a bedding fault: Understanding the initiation and movement of the Daguangbao landslide triggered by the 2008 Wenchuan Earthquake (Ms = 8.0). *Eng. Geol.* 295, 106455. doi:10.1016/j.enggeo.2021.106455

Divoux, P., Boulon, M., and Bourdarot, E. (1997). A mechanical constitutive model for rock and concrete joints under cyclic loading. *Proc. Damage Fail. Interfaces*, 443–450.

Dong, S., Feng, W., Yin, Y., Hu, R., and Zhang, G. (2020). Calculating the permanent displacement of a rock slope based on the shear characteristics of a structural plane under cyclic loading. *Rock Mech. Rock Eng.* (53), 4583–4598. doi:10.1007/s00603-020-02188-y

Fathi, A., Moradian, Z., Rivard, P., and Ballivy, G. (2016). Shear mechanism of rock joints under pre-peak cyclic loading condition. *Int. J. Rock Mech. Min. Sci.* 83, 197–210. doi:10.1016/j.ijrmms.2016.01.009

Fox, D. J., Kan, D. D., and Hsiung, S. M. (1998). Influence of interface roughness on dynamic shear behavior in jointed rock. *Int. J. Rock Mech. Min. Sci.* 35 (7), 923–940. doi:10.1016/s0148-9062(98)00153-3

Fw, A., Jie, W. B., Han, B. C., Bo, L. A., Zs, D., and Dk, E. (2021). Advances in statistical mechanics of rock masses and its engineering applications. *J. Rock Mech. Geotechnical Eng.* 13 (1), 22–45. doi:10.1016/j.jrmge.2020.11.003

Goldstein, M., Goosev, B., Pvrogovsky, N., Tulinov, R., and Turovskaya, A. (1966). Investigation of mechanical properties of cracked rock. *Surf. Rev. Lett.* 7 (7), 667–671.

Han, D., Leung, Y. F., and Zhu, J. (2022). Tensile strength and deformational behavior of stylolites and mineral healed joints subject to dynamic direct tension. *Rock Mech. Rock Eng.* 55 (4), 1997–2009. doi:10.1007/s00603-021-02730-6

Homand, F., Belem, T., and Souley, M. (2001). Friction and degradation of rock joint surfaces under shear loads. *Int. J. Numer. Anal. Methods Geomech.* 25 (10), 973–999. doi:10.1002/nag.163

Hu, J., Li, S., Liu, H., Li, L., and Qin, C. (2020). New modified model for estimating the peak shear strength of rock mass containing nonconsecutive joint based on a simulated experiment. *Int. J. Geomech.* 20 (7), 04020091. doi:10.1061/(asce)gm.1943-5622.0001732

Huang, R., and Li, W. (2009). Development and distribution of geohazards triggered by the 5.12 Wenchuan Earthquake in China. *Sci. China Ser. E-Technol. Sci.* 52 (4), 810–819. doi:10.1007/s11431-009-0117-1

Huang, X., Haimson, B. C., Plesha, M. E., and Qiu, X. (1993). An investigation of the mechanics of rock joints-Part I. Laboratory investigation. *Int. J. Rock Mech. Min. Sci. Geomechanics Abstr.* 30 (3), 257–269. doi:10.1016/0148-9062(93)92729-a

Hutson, R. W., and Dowding, C. H. (1990). Joint asperity degradation during cyclic shear. *Int. J. Rock Mech. Min. Sci. Geomechanics Abstr.* 27 (2), 109–119. doi:10.1016/0148-9062(90)94859-r

Jafari, M. K., Hosseini, K. A., Pellet, F., Boulon, M., and Buzzi, O. (2003). Evaluation of shear strength of rock joints subjected to cyclic loading. *Soil Dyn. Earthq. Eng.* 23 (7), 619–630. doi:10.1016/s0267-7261(03)00063-0

Jing, L., Stephansson, O., and Nordlund, E. (1993). Study of rock joints under cyclic loading conditions. *Rock Mech. Rock Eng.* 26 (3), 215–232. doi:10.1007/bf01040116

Lee, H. S., Park, Y. J., Cho, T. F., and You, K. H. (2001). Influence of asperity degradation on the mechanical behavior of rough rock joints under cyclic shear loading. *Int. J. Rock Mech. Min. Sci. (1997).* 38 (7), 967–980. doi:10.1016/s1365-1609(01)00060-0

Li, H. (2022). SCADA data based wind power interval prediction using LUBE-based deep residual networks. *Front. Energy Res.* 10, 920837. doi:10.3389/fenrg.2022.920837

Li, H. (2022). Short-term wind power prediction via spatial temporal analysis and deep residual networks. *Front. Energy Res.* 10, 920407. doi:10.3389/fenrg.2022.920407

Li, H., Deng, J., Feng, P., Pu, C., Arachchige, D., and Cheng, Q. (2021). Short-term nacelle orientation forecasting using bilinear transformation and ICEEMDAN framework. *Front. Energy Res.* 9, 780928. doi:10.3389/fenrg.2021.780928

Li, H., Deng, J., Yuan, S., Feng, P., and Arachchige, D. (2021). Monitoring and identifying wind turbine generator bearing faults using deep belief network and EWMA control charts. *Front. Energy Res.* 9, 799039. doi:10.3389/fenrg.2021.799039

Liu, B., Li, H., Liu, Y., and Xia, X. (2013). Generalized damage model for asperity and shear strength calculation of joints under cyclic shear loading. *Chin. J. Rock Mech. Eng.* 32 (2), 3000–3008.

Liu, B., Li, H., and Zhu, X. (2011). Experiment simulation study of strength of degradation of rock joints under cyclic shear loading. *Chin. J. Rock Mech. Eng.* 30 (10), 2033–2039.

Liu, Y. (2017). *Study on cumulative damage evolution mechanism and stability of bedding rock slope in reservoir area under frequent microseismic*. Chongqing: Chongqing University.

Mirzaghorbanali, A., Nemcik, J., and Aziz, N. (2014). Effects of shear rate on cyclic loading shear behaviour of rock joints under constant normal stiffness conditions. *Rock Mech. Rock Eng.* 47 (5), 1931–1938. doi:10.1007/s00603-013-0453-0

Moriya, H., Abe, S., Ogita, S., and Higaki, D. (2010). Structure of the large-scale landslide at the upstream area of aratozawa dam induced by the iwate-miyagi nairiku earthquake in 2008. *J. Jpn. Landslide Soc.* 47 (2), 77–83. doi:10.3313/jls.47.77

Mroz, Z., and Giambanco, G. (2015). An interface model for analysis of deformation behaviour of discontinuities. *Int. J. Numer. Anal. Methods Geomech.* 20 (1), 1–33. doi:10.1002/(sici)1096-9853(199601)20:1<1::aid-nag799>3.0.co;2-l

Newland, P. L., and Allely, B. H. (1957). Volume changes in drained taixial tests on granular materials. *Geotechnique* 7 (1), 17–34. doi:10.1680/geot.1957.7.1.17

Patton, F. D. (1966b). Multiple modes of shear failure in rock. *Proceeding the1st Congr. Int. Soc. Rock Mech.* 1, 509–513.

Patton, F. D. (1966a). *Multiple modes of shear failure in rock and related materials*. Illinois: University of Illinois.

Plesha, M. E. (1987). Constitutive models for rock discontinuities with dilatancy and surface degradation. *Int. J. Numer. Anal. Methods Geomech.* 11 (4), 345–362. doi:10.1002/nag.1610110404

Premadasa, W., Indraratna, B., Mizargobanali, A., and Oliveira, D. (2012). *Shear behaviour of rock joints under cyclic loading. Australia-New Zealand conference on geomechanics: Ground engineering in A changing world*.

Qiu, X., Plesha, M., Huang, X., and Haimson, B. (1993). An investigation of the mechanics of rock joints-Part II. Analytical investigation. *Int. J. Rock Mech. Min. Sci. Geomechanics Abstr.* 30 (3), 271–287. doi:10.1016/0148-9062(93)92730-e

Qu, J. (2018). *Experimental study on shear characteristics of rock joints under cyclic loading*. Dissertation: Chongqing University.

Siad, L. (2003). Seismic stability analysis of fractured rock slopes by yield design theory. *Soil Dyn. Earthq. Eng.* 23 (3), 21–30. doi:10.1016/s0267-7261(02)00213-0

Wang, S., and Zhang, J. (1982). Dynamic analysis of sliding stability of slope rock mass. *Chin J Geol* 2, 162–170.

Woo, I., Fleurisson, J. A., and Park, H. J. (2010). Influence of weathering on shear strength of joints in a porphyritic granite rock mass in Jechon area, South Korea. *Geosci. J.* 14 (3), 289–299. doi:10.1007/s12303-010-0026-0

Xia, C., Song, Y., Tang, Z., and Shou, C. (2012). Particle flow numerical simulation for shear behavior of rough joints. *Chin. J. Rock Mech. Eng.* 31 (8), 1545–1552.

Xie, S., Lin, H., Cheng, C., Chen, Y., Wang, Y., Zhao, Y., et al. (2022). Shear strength model of joints based on Gaussian smoothing method and macro-micro roughness. *Comput. Geotechnics* 143, 104605. doi:10.1016/j.compgeo.2021.104605

Xu, J., Liu, Y., Yin, G., Li, B., and Ye, G. (2015). Development of shear-flow coupling test device for coal rock. *Chin. J. Rock Mech. Eng.* 34, 2987–2995.

Zhang, X., Ren, M., Meng, Z., Zhang, B., and Li, J. (2021). Experimental study on the mechanical behavior of yunnan limestone in natural and saturated states. *Adv. Civ. Eng.*, 1–16. doi:10.1155/2021/6614412

Zhou, J., Wei, J., Yang, T., Zhang, P., Liu, F., and Chen, J. (2021). Seepage channel development in the crown pillar: Insights from induced microseismicity. *Int. J. Rock Mech. Min. Sci.* 145, 104851. doi:10.1016/j.ijrmms.2021.104851